PROTON ACCELERATION DRIVEN BY HIGH ENERGY DENSITY ELECTRONS

S. Zhao, J. E. Chen, School of Physical Sciences, UCAS, Beijing, 100191 China and
State Key Laboratory of Nuclear Physics and Technology and
CAPT, Peking University, Beijing, 100871 China.
C. Lin†, H. Y. Wang,B. Liu, Y. X. Geng, H. Z. Fu, Y. R. Lu, X. T. He, X. Q. Yan‡,
State Key Laboratory of Nuclear Physics and Technology and CAPT,
Peking University, Beijing, 100871, China.

Abstract

Proton acceleration driven by resonance electrons, which are generated through direct laser acceleration in the near critical dense plasma, is proposed. These energetic electron beam is dense and directional. When interacting with a thin foil target, resonance electrons can transmit the target and drive periodical electrostatic field at the back surface with a much longer scale length than the classical target normal sheath field. Therefore protons are more efficiently accelerated in propagation direction of resonance electrons. For a Gaussian laser pulse with pulse duration of $80fs$ and peak intensity $I_0 = 1.38\times10^{18}W/cm^2$, the cutoff energy of the output collimated proton beam is 14 MeV, enhanced by a factor of 4. The scaling law predicts proton beam over 100 MeV energy can be generated in laser intensity of $10^{20}W/cm^2$.

INTRODUCTION

Near critical plasma has been used to improve the energy coupling efficiency of intense relativistic laser into plasma, in which laser pulse channels due to relativistic and ponderomotive effects[1, 2] and transfer its energy into plasma electrons. For example, Bulanov et al.[3] reported that energetic ions are accelerated at the rear surface of near critical plasma by magnetic vortex. Wang et al.[4] and Sgattoni et al.[5] also reported the improvement of proton cutoff energy by combining a near critical density gas plasma in front of a solid target.

we report a novel mechanism of proton acceleration driven by resonance electrons. A gas-foil combination target is used. The energetic RE are first generated in the near critical gas plasma, then penetrate the thin foil target and form a periodical electrostatic field at the back surface of the foil, as shown in Fig 1. The protons are effectively accelerated by the field and the cutoff energy is 4 times higher compared to the classical target normal sheath acceleration.

PIC SIMULATION

2D relativistic simulation code KLAP[6] is used to investigate more insight of the RE driven ion acceleration. The simulation length, time, charge, mass and density are normalized to laser wavelength $\lambda_0 = 1.06\mu$m, laser period T, electron charge e, electron mass m_e and the critical density $n_c = m_e\varepsilon_0{\omega_0}^2/e^2$, respectively. The simulation box is $80\lambda_0 \times 40\lambda_0(z \times y)$ while z direction is the target normal direction. Simulation begins at 0T and stops at 200T. The target structure is the same as shown in Fig 1. The gas plasma layer is located from 5μm to 25μm with a H plasma density of $0.125n_c$. The foil target is composed by a Al^{3+} plasma with $90n_c$ density and 1.0μm thickness, together with two H layers attached at both front and back surfaces with $10n_c$ density and 0.1μm thickness. The initial temperatures are 500 eV for electrons and ions. The laser pulse is p-polarized(y direction)and has Gaussian distribution in both space and time with the normalized vector potential $a = 1.0\times exp(-(r/\sigma_0)^2 - ((t-80)/48)^2)$ ($a = eA_L/m_ec$, and $a = 1.0$ corresponds to $I/{\lambda_0}^2 = 1.38\times10^{18}W/cm^2\mu m^2$), where the pulse duration is 264fs and the focal radius $\sigma_0 = 6\lambda_0$.

Table 1: Simulation parameters

Laser	Values	Target	Values
a(normalized)	1	Density of gas	$0.2N_c$
Focal spot	$5\mu m$	thick of gas	20μm
Incident angle	$45°$	Density of foil	$0.2N_c$
Duration	$264fs$	thick of gas	20μm
Envelope	Gaussian	Density of H	$0.2N_c$

ION ACCELERATION

The analysis of Acceleration

Fig 2.(a) shows the electric field distribution at t= 100T, in which two kind of field are clearly distinguishable, the periodic field E_{RE} generated by RE and the dispersed field E_{sheath} from sheath electrons. In Fig 2.(b), the blue line is the line-out of electric field strength E_{acc} along the arrow line shown in Fig 2.(a). The peak around z= 26.2μm is from the E_{sheath} and the following periodical structures is from E_{RE}. The red line and blue line are well coincident except for the E_{sheath} peak at z= 26.2μm because of the target normal sheath field. In the simulation, ions at the rear surface of the foil are first accelerated by E_{sheath}, then only those located at the RE beam passing area can be captured by E_{RE} and further accelerated along the RE direc-

* Work supported by National Basic Research Program of China (Grant No. 2013CBA01502) and National Natural Science Foundation of China (Grant Nos. 11025523, 10935002, 10835003, J1103206)
† linchen0812@pku.edu.cn
‡ x.yan@pku.edu.cn

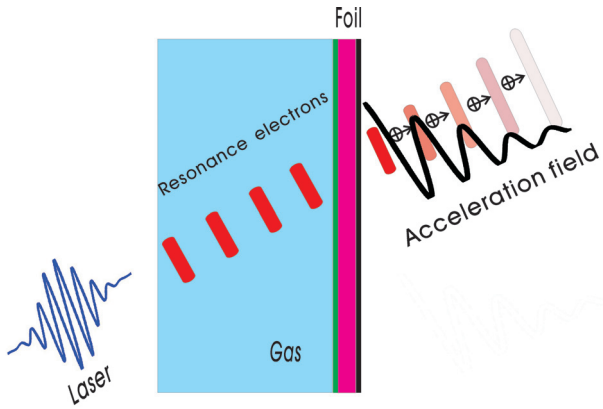

Figure 1: (Color online) Configuration of the simulation. The laser (blue) pulse incidents obliquely in 45° on the gas plasma (blue). Resonance electrons beam (red) are generated in the gas and interact with the $90n_c$ $1.0\mu m$ Aluminum foil attached with $10n_c$ $0.1\mu m$ H layers at both the front (green) and back (black) surfaces

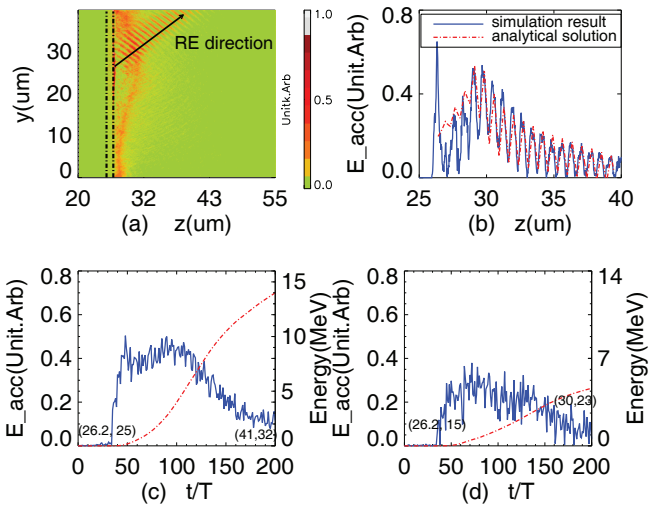

Figure 2: (Color online) Acceleration field information at t= 100T(typical), 2D distribution of acceleration field E_{acc} (a), 1D slice of E_{acc} along the RE direction and the analytical result (b). Time evolution of energy gain and witnessed field for the proton captured in E_{RE}(c) and for the uncaptured proton(d).

tion. Two test protons are traced in the simulation: particle '1' is initially at (26.2, 25) and '2' is at (26.2, 15). The time dependence of the energy and witnessed field for the test protons are depicted in Fig 2(c) and Fig 2(d). Both E_{sheath} and E_{RE} start at t= 30T when the laser and RE bunches reach the target. After the acceleration of E_{sheath}, particle '1' is captured in E_{RE} again and further accelerated while '2' not. For '1', the strongest E_{RE} is at about t= 100T when the RE are the most energetic. Finally at t= 200T '1' gains 14MeV in 15.5μm acceleration distance while '2' only achieves 4MeV in 8.8μm. Due to the stronger and longer acceleration field, particle '1' gains much higher energy. Therefore RE driven proton acceleration dominates sheath acceleration here.

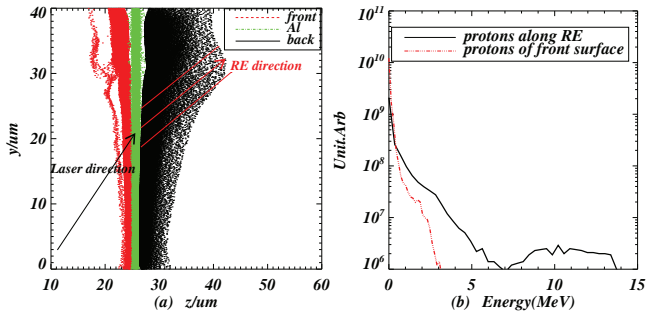

Figure 3: (Color online) The ions information at $t = 200$T. (a)Ion spatial distribution, black for protons at the back surface, green for Al ions, red for protons at the front surface;(b)proton energy spectrum, protons at the back surface(black) are accumulated in the area along the RE direction as depicted in (a); red for protons in the front surface.

Proton Beam Quality

The snapshots of ion acceleration at t= 200T are illustrated in Fig 3. Fig 3.(a) is the spatial distribution of Al^{3+}(green), protons at the front(red) and rear surfaces(black). It shows that most of the faster protons fly in the RE direction(framed with red lines with width equal to the RE bunch diameter) at the rear side, indicating RE driving proton acceleration through E_{RE} dominates over TNSA. Fig 3.(b) shows the energy spectrum for the front surface proton(red) and for the back surface protons accumulated along the RE direction(black). The cutoff energy is 4MeV for the front surface protons, consistent with the TNSA energy equation $E_{max} = 2T_{hot}[In(t_p + (t_p{}^2 + 1)^{1/2})]^2$ [8](where T_{hot} is the electron temperature, t_p is the effective acceleration time). While for RE driving protons, the cutoff energy is 14MeV, which is about 3.5 times higher than the front protons. The more effective acceleration along the RE direction is due to the longer and stronger acceleration field E_{RE}. Meanwhile the energy spread is improved since the E_{RE} is periodically decreasing, higher energy protons which move faster into weaker field and gain less energy according to Fig 2.(b), so the energy difference between protons are reduced. Hence the protons along the RE direction are mono-energetic as Fig 3.(b) shows.

THE OPTIMUM CONDITION

In order to test the robustness of this acceleration mechanism, the laser intensity and the plasma density are scanned in simulations. The normalized laser amplitude a is varied from 1.0 to 11.0 with step 2.0 and the density is from $0.1n_c$ to $0.8n_c$. Fig 4(a) is the dependence of the proton cutoff energy on the laser intensity and plasma density. Effective acceleration can be achieved by matching the laser amplitude and the density(keeping the plasma skin length

ISBN 978-3-95450-122-9

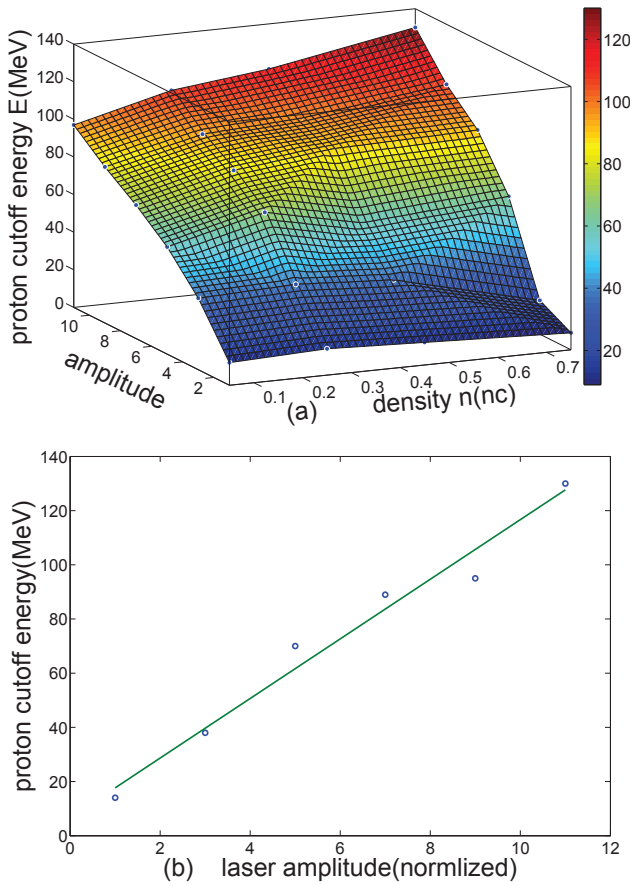

Figure 4: (Color online)(a) The proton cutoff energy versus the laser intensity and foam density. The laser amplitude varies from 1 to 11.0 while the density from $0.125n_c$ to $2.0n_c$. (b)proton energy versus laser amplitude while keeping the plasma skin length as constant.

$l_s/\lambda = \sqrt{an_c/n_e}$ as constant). In Fig 4(b) shows the proton energy scales with laser amplitude if keeping the plasma skin length.

CONCLUSION

To summarize, a novel scheme for proton acceleration by resonance electrons in near critical gas plasma is proposed. The RE have higher temperature and smaller divergence than the $J \times B$.[9] heating electrons. Periodical field E_{RE} driven by the RE at the target rear is effective for ion acceleration since the field is stronger and longer than sheath field. Energetic protons with 14MeV cutoff energy is got in case of laser pulse with duration of 80fs, peak intensity of $1.38\times10^{18}W/cm^2$, which is 3 to 4 times higher than TNSA. Hundreds of MeV protons are expected at laser intensity of $10^{20}W/cm^2$ by the scaling law while the ultra-high contrast and steepened pulse profile with a very short rise time are not necessary here, which is promising for compact proton cancer therapy system in the near future.

ACKNOWLEDGMENT

This work was supported by National Natural Science Foundation of China (Grant Nos. 11025523,10935002,10835003,J1103206) and National Basic Research Program of China (Grant No. 2011CB808104).

REFERENCES

[1] A. B. Borisov, O. B. Shiryaev, A. McPherson et al., Plasma Phys. Controlled Fusion 37, 569 (1995). M. Borghesi, A. J. MacKinnon, L. Barringer et al., Phys. Rev. Lett 78, 879 (1997)

[2] A. Pukhov, J. Meyer-ter-Vehn, Phys. Rev. Lett 76, 3975 (1996). A. Pukhov, Z. M. Sheng, J. Meyer-ter-Vehn , Phys.Plasmas 6, 2847 (1999).

[3] Stepan S. Bulanov, Valery Yu. Bychenkov, Vladimir Chvykov et al., Phys. Plasmas 17, 043105 (2010)

[4] H. Y. Wang, C. Lin, F. L. Zheng et al., Phys. Plasmas 18, 093105 (2011)

[5] A. Sgattoni, P. Londrillo, A. Macchi et al., Phys. Rev. E 85, 036405 (2012).

[6] Zheng-Ming Sheng, Kunioki Mima, Jie Zhang et al., Phys. Rev. Lett 94, 095003 (2005).

[7] Hiroyuki Daido, Mamiko Nishiuchi and Alexander S Pirozhkov, Rep. Prog. Phys 75, 056401 (2012).

[8] P. Mora, Phys. Rev. Lett 90, 185002 (2003).

[9] W. L. Kruer and Kent Estabrook, Phy.Fluids 28, 430 (1985).